Supplemental information

Short description of the program 'ELcalc' (**effective length calculation**):

The tensor of the moment of inertia was calculated according to Meschede (*1*) using the coordinates from the X-ray structure and masses of the atoms of a particular chromophore. The eigenvectors of this tensor are the main axis of inertia of this chromophore. They are determined by diagonalizing this tensor using a standard algorithm. The conjugated system of double bonds determined from the chemical structure of the chromophore was projected onto the eigenvector (of length 1 Å) with the lowest eigenvalue. The extension of this projection is the effective length (in Å).

Literature supplemental information

1. Meschede, D. (2004) *Gerthsen Physik*, Springer p. 77.

2. Ritter, S., Hiller, R. G., Wrench, P. M., Welte, W., and Dieterich, K. (1999) Crystal structure of a phycourobilin-containing phycoerythrin at 1.9 Å resolution, *J. Struct. Biol. 126*, 86.

3. Sidler, W. A. (1994) Phycobilisome and Phycobiliprotein Structures. In: *The Molecular Biology of Cyanobacteria* (Bryant D. A., Ed.), pp. 139 ff, Kluwer Academic Publishers, Dortrecht.

4. Doust, A. B., Marai, C. N., Harrop, S. J., Wilk, K. E., Curmi, P. M., and Scholes, G. D. (2004) Developing a structure-function model for the cryptophyte phycoerythrin 545 using ultrahigh resolution crystallography and ultrafast laser spectroscopy. *J. Mol. Biol.* **344**, 135.

5. Wedemayer, G. J., Kidd, D. G., Wemmer, D. E., and Glazer, A. N. (1992) Phycobilins of cryptophycean algae, *J. Biol. Chem*. *267***,** 7315-7331.

6. Schmidt, M., Krasselt, A., and Reuter, W. (2006) Local protein flexibility as a prerequisite for reversible chromophore isomerization in α-Phycoerythrocyanin, *Biochim. Biophys. Acta 1764***,** 55-62.

7. Zhao, K.-H., and Scheer, H. (1995) Type I and type II reversible photochemistry of phycoerythrocyanin α-subunit from *Mastigocladus laminosus* both involve *Z*, *E* isomerization of phycoviolobilin chromophore and are controlled by sulfhydryls in apoprotein, *Biochim. Biophys. Acta 1228*, 244-253.

8. Nield, J., Rizkallah, R. J., Barber, J., and Chayen, N. E. (2003) The 1.45 Å three dimensional structure of C-Phycocyanin from the thermophilic cyanobacterium *Synechococcus elongates*, *J. Struct. Biol. 141*, 149-155.

9. MacColl, R. (1998) Cyanobacterial Phycobilisomes, *J. Struct. Biol. 124*, 311-334.

10. Reuter, W., Wiegand, G., Huber, R., and Than, M. E. (1999) Structural analysis at 2.2Å of orthorhombic crystals present the asymmetry of the allophycocyanin-linker complex, $AP{\cdot}L_C^{7.8}$, from phycobilisomes of *Mastigocladus laminosus*, *Proc. Natl. Acad. Sci. USA 96*, 1363-1368.

11. Demidov, A. A., and Mimuro, M. (1995) Deconvolution of C-Phycocyanin β-84 and β-155 Chromophore Absorption and Fluorescence Spectra of Cyanobacterium *Mastigocladus laminosus*, *Biophys J. 68*, 1500-1506.

12. Wagner, J. R., Brunzelle, J. S., Forest, K. T., and Vierstra, R. D. (2005) A light-sensing knot revealed by the structure of the chromophore-binding domain of phytochrome, *Nature 438*, 325-331.

13. Karniol, B., Wagner, J. R., Walker, J. M., and Vierstra, R. D. (2005) Phylogenetic analysis of the phytochrome superfamily reveals distinct microbial subfamilies of photoreceptors, *Biochem. J. 392*, 103-116.

14. Cornejo, J., Beale, S. I., Terry, M. J., and Lagarias, C. (1992) Phytochrome Assembly, *J. Biol. Chem. 267*, 14790-14798

15. Batschauer, A. (1998) Photoreceptors of higher plants, *Planta 206*, 479-492.

16. Carson, M. (1997) Ribbons, in *Methods in Enzymology* (Sweet, R. M, and Carter C. W. Eds.) Vol. 277, pp. 493-505, Academic Press, New York.

17. McRee, D. E. (1999) "XtalView/Xfit - A Versatile Program for Manipulating Atomic Coordinates and Electron Density", *J. Structural Biology 125***,** 156-165.

Table S1. Effective length and absorption of different bilins. References are given for the pdb-entry and the spectral absorption.

Chromophore	protein	organism	pdb-entry	effective length [Å]	absorption [nm]	remark
PUB	PE	*G. monilis*	1B8D (*2*)	5.66	495 (*3*)	average from literature
^{15}E-PVB	PEC	*M. laminosus*		6.12	504	α_E-PEC, this work
PEB α 82 PEB α 139 PEB β 158	PE	*G. monilis*	1B8D (*2*)	9.40 9.10 9.46	548 (*3*)	average from literature
DBV	PE	*Rhodomonas sp.*	1XF6 (*4*)	10.81	562 (*5*)	$(\alpha_1\beta)(\alpha_2\beta)$-dimer
^{15}Z-PVB	PEC	*M. laminosus*	2C7L (*6*)	11.07	568 (*7*)	α_Z-PEC
PCB β153	PEC	*M. laminosus*	2C7L (*6*)	13.46	592#	isolated β-subunit
PCB β84	PEC	*M. laminosus*	2C7L (*6*)	14.13	604#	isolated β-subunit
PCB α84	PC	*S. elongatus*	1JBO (*8*)	14.86	624 (*9*) 610#	(αβ)-trimer* isolated α-subunit
PCB β84	PC	*S. elongatus*	1JBO (*8*)	14.62	628 (*9*) 618#	(αβ)-trimer* isolated β-subunit
PCB β155	PC	*S. elongatus*	1JBO (*8*)	14.97	600 (*9*)	(αβ)-trimer
PCB β84	AP	*M. laminosus*	1B33 (*10*)	14.57	650 (*11*) 615#	(αβ)-trimer* isolated β-subunit
PCB α82	AP	*M. laminosus*	1B33 (*10*)	14.70	652 (*11*) 615#	(αβ)-trimer* isolated α-subunit
BV	bacterial phytochrome	*D. radiodurans*	1ZTU (*12*)	not done	696 (*13*)	curved Syn/Syn/Anti configuration
$P\Phi B_r$ (^{15}Z)	Phytochrome	plant		14.93	660 (*14,15*)	modelled on ^{15}E-PVB
$P\Phi B_{fr}$ (^{15}E)	Phytochrome	plant		16.24	720 (*14,15*)	modelled on ^{15}Z-PVB

own measurements
*: excitonically coupled

Table S2. Selected interactions identified in the $\alpha_{E1}\alpha_{E2}$ homodimer and its artificial ring compared to those found in the native $(\alpha\beta)_3$-PEC. The nomenclature of the subunits is explained in the text.

αα-PEC and artificial $(\alpha_\alpha\alpha_\beta)_3$ ring		distance [Å]
$\alpha_{\alpha(N)}$-$\alpha_{\beta(N)}$ interactions (asymmetric unit)		
α_αTyr18 O_η- α_βAsp89 $O_{\delta2}$	hydrogen bond	3.0
α_αAsp89 $O_{\delta2}$- α_βTyr18 O_η	hydrogen bond	3.0
α_αTyr97 O_η- α_βSer17 O	hydrogen bond	2.5
α_αSer17 O - α_βTyr97 O_η	hydrogen bond	2.5
$\alpha_{\beta(N)}$-$\alpha_{\beta(N+1)}$		
none, α_βThr77 instead of βHis75		**
$\alpha_{\beta(N)}$-$\alpha_{\alpha(N+1)}$ interactions		
βLys81 N_ζ – αPVB O_{89}	hydrogen bond	3.3 **
native $(\alpha\beta)_3$-PEC		
α_N-β_N interactions (asymmetric unit)		
αThr3 O- βAsp3 O_δ	hydrogen bond	2.6
αAsp13 $O_{\delta2}$ - βTyr92 O_η	hydrogen bond	2.7
αSer17 O - βTyr95 O_η	hydrogen bond	2.7 *
αTyr97 O_η - βAla17 O	hydrogen bond	2.6 *
αTyr18 - βPCB 153, ring D	π-Stack	4.5
αTyr18 O_η - βArg91 N	hydrogen bond	3.3 *
αAsp89 $O_{\delta2}$ - βTyr18 O_η	hydrogen bond	3.0 *
αArg35 N_ε- βGln28 $O_{\varepsilon1}$	hydrogen bond	3.0 *
αArg42 $N_{\eta1}$-βAsn25 $O_{\delta1}$	hydrogen bond	2.8 *
β_N-β_{N+1} interactions		
βHis75 N_ε-βAsp13 $O_{\delta1}$	hydrogen bond	2.7 *
β_N-α_{N+1} interactions		
βHis 76N_δ- αVal 111 O	hydrogen bond	2.8 *
βHis 76 - αTyr 110	π-Stack	4.5
βHis 76 – αPVB ring D	π-Stack	4.0
βArg75 N_ε-αPVB O_{84}	hydrogen bond	3.1 *
βGln79 $O_{\varepsilon2}$-αPVB O_{19}	hydrogen bond	3.2 *
βHis75 N_δ – αPVB O_{19}	hydrogen bond	2.9 *
βArg75 $N_{\eta2}$-αLeu122 O	hydrogen bond	2.9 *
* important for ring formation ** missing interactions prevent ring stability/formation		

Table S3. Distances across symmetry related subunits near the chromophore for subunit α_{E1} (A) and α_{E2} (B).

Distances between subunits related by symmetry in [Å]	
subunit α_{E1}	
A84 PVB O_{84} - B125 Ser O_{γ}	2.6
A84 PVB O_{89} – A83 Lys N_{ζ}	2.5
A84 PVB O_{90} – B76 Tyr O_{η}	3.0
A83 Lys N_{ζ} - B124 Gly O	3.3
subunit α_{E2}	
B84 PVB O_{84} – A125 Ser O_{γ}	3.5
B84 PVB O_{90} – A83 Lys N_{ζ}	2.8
B84 PVB O_{90} – A76 Tyr O_{η}	3.3
B83 Lys N_{ζ} - A124 Gly O	2.5

Figure legends supplemental material

Figure S1. Chemical structures of different bilins with examples of occurrence in biliproteins and organisms. The number (N) of conjugated bonds is given and highlighted in colour on top of the structures. (A) PUB: phycourobilin in phycoerythrin of *G. monilis*. (B) Two different configurations of phycoerythrobilin ring A are shown; the isomer on the right side extends the conjugated system into ring A. (C) PEB: phycoerythrobilin in phycoerythrin of *G. monilis*. (D) DBV: Dihydrobiliverdin in phycoerythrin of *Rhodomonas sp. CS24*. (E) PVB: phycoviolobilin in phycoerythrocyanin of *M. laminosus*. (F) PCB: Phycocyanobilin in

phycoerythrocyanin, phycocyanin and allophycocyanin of *M. laminosus*. The main axes of inertia are indicated by the arrows. (G) PΦB: Phytochromobilin in plant phytochromes. (H) BV: Biliverdin in bacterial phytochrome of *D. radiodurans*. (I) The nomenclature for an extended chromophore geometry is shown for a torso chromophore. Double bonds Δ4,5, Δ10,11 and Δ15,16 are all in the *Z*-configuration, however, ring B is anti to ring A, ring C syn to ring B and ring D anti to ring C.

Figure S2. The $\alpha_E\alpha_E$-dimer as it is lying in the asymmetric unit (stereo-representation). The electron density of the ^{15}E-PVB chromophore is highlighted in pink. a) Front view, the 9 helices and the chromphores are clearly visible. b) The side view shows how the N-terminal helices interact. (figure prepared with 'ribbons', ref. *16*)

Figure S3. Structure of the near environment of the chromophores across the borders of subunits related by symmetry. Interactions are shown by the dotted lines. Subunits in the asymmetric unit are shown in yellow, those related by symmetry in purple. a) close-up on phycoviolobilin in α_{E1}, b) close-up on phycoviolobilin in α_{E2}, c) larger view on subunit α_{E1} including Tyr110, dotted arrow: prospective pathway to the water bound to the ring D nitrogen. d) same as in c) but for subunit α_{E2} (figure prepared with 'xfit', ref. 17)

- figure S1 –

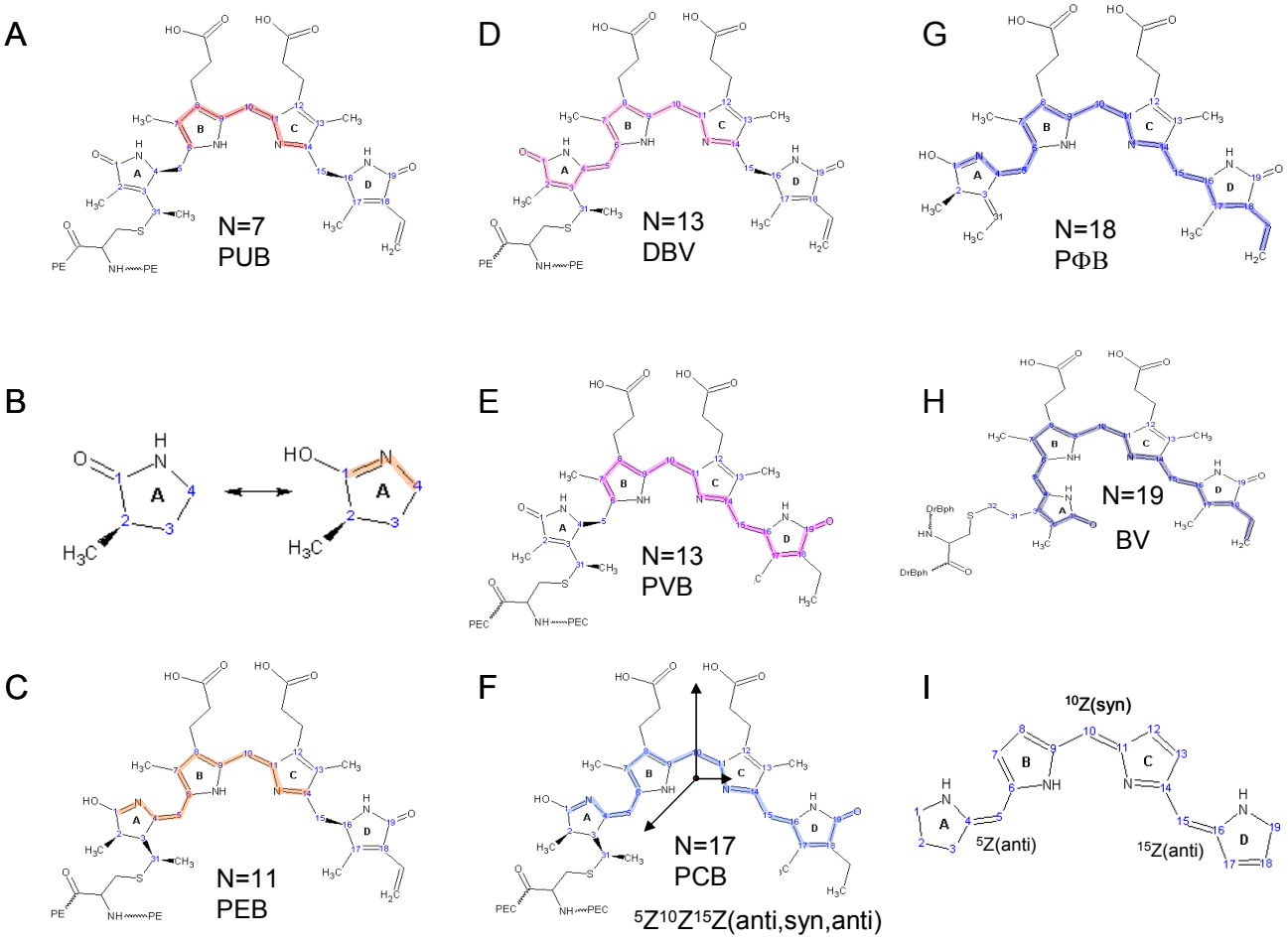
A
N=7
PUB
D
N=13
DBV
G
N=18
PΦB
B
E
N=13
PVB
H
N=19
BV
C
N=11
PEB
F
N=17
PCB
5Z10Z15Z(anti,syn,anti)
I
10Z(syn)
5Z(anti)
15Z(anti)

- figure S2 -

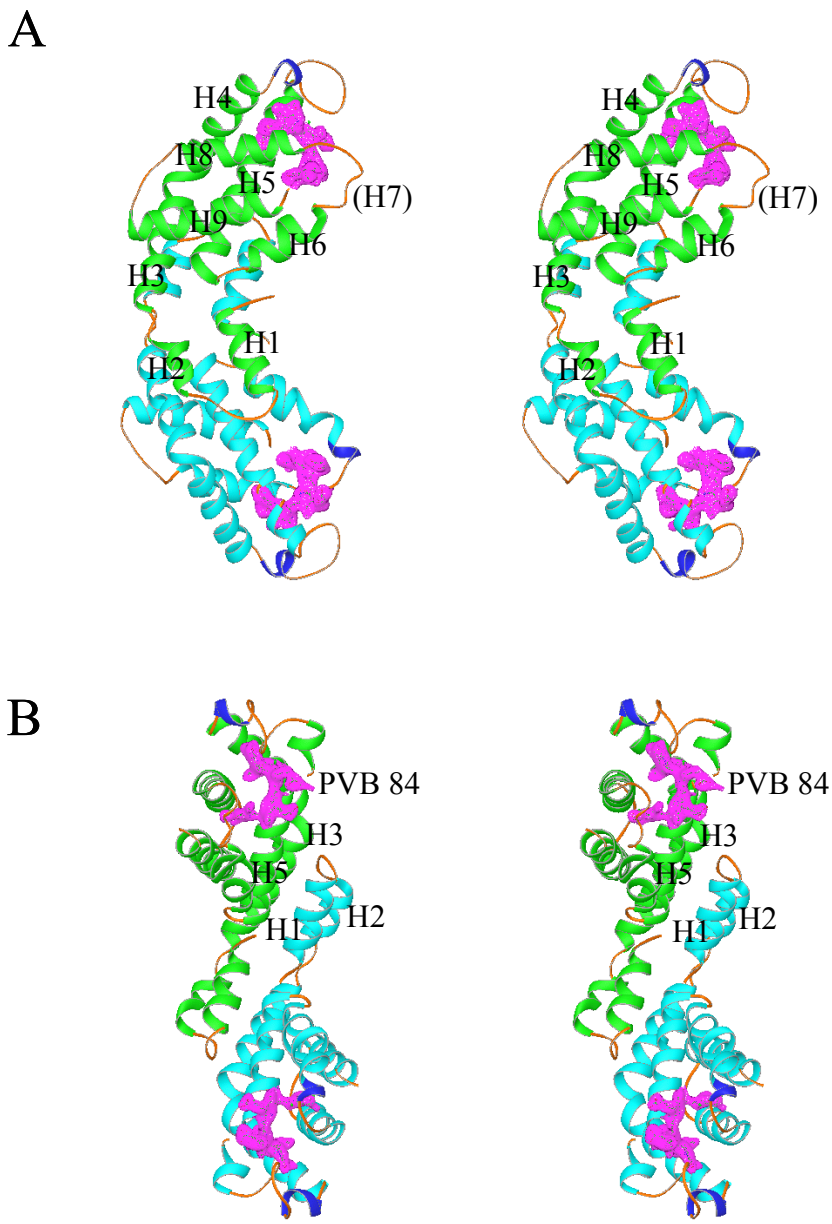
A
H4
H8
H5
(H7)
H9
H6
H3
H1
H2
H4
H8
H5
(H7)
H9
H6
H3
H1
H2
B
PVB 84
H3
H5
H1
H2
PVB 84
H3
H5
H1
H2

- figure S3 -

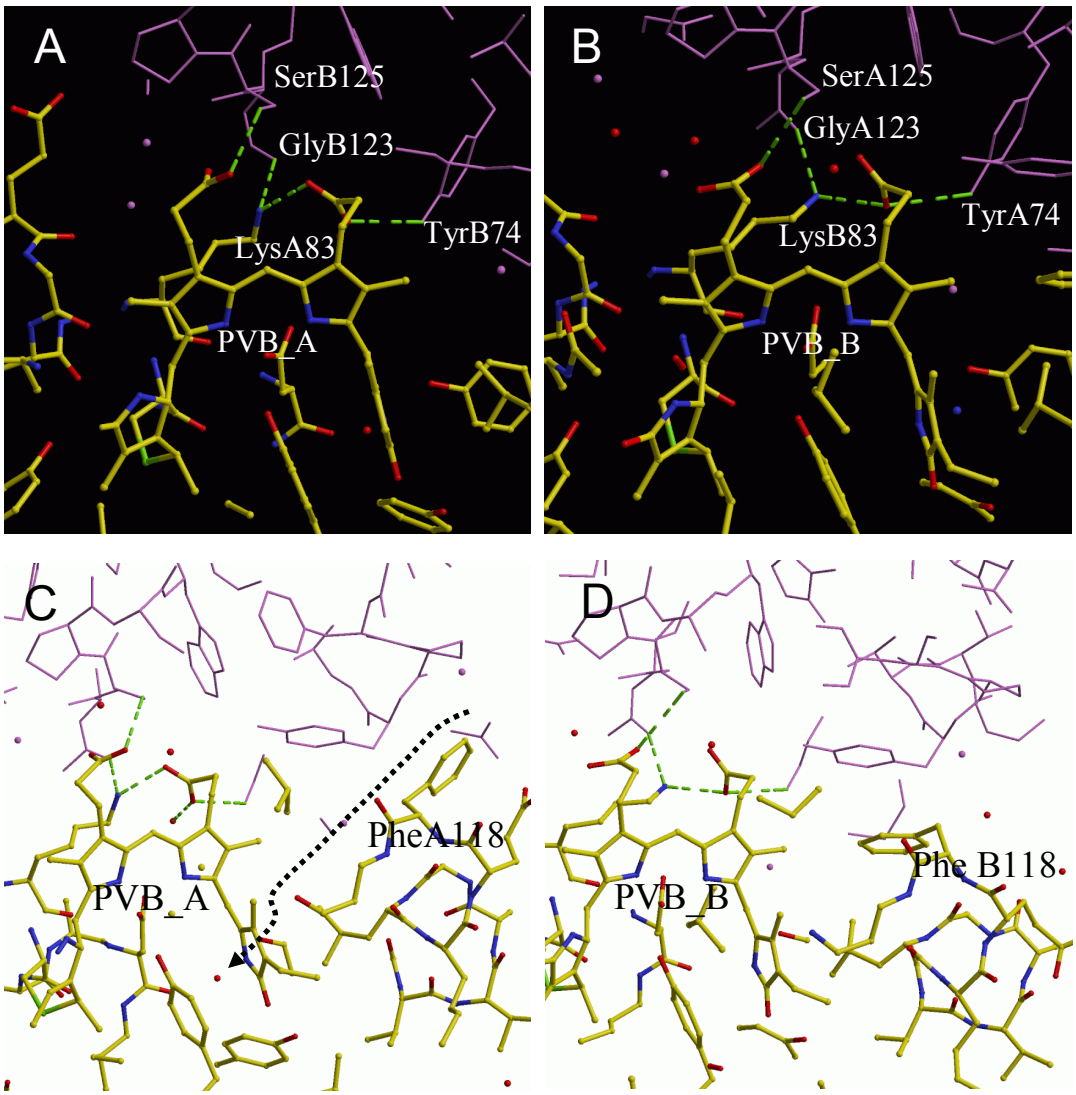
A
SerB125
GlyB123
TyrB74
LysA83
PVB_A
B
SerA125
GlyA123
TyrA74
LysB83
PVB_B
C
PheA118
PVB_A
D
Phe B118
PVB_B